Research on Biomedical Engineering
https://doi.org/10.1007/s42600-019-00028-9

ORIGINAL ARTICLE

Automatic segmentation of blood vessels in retinal images using 2D Gabor wavelet and sub-image thresholding resulting from image partition

Luciana da Silva Amorim[1] · Flávia Magalhães Freitas Ferreira[1] · Juliana Reis Guimarães[2] · Zélia Myriam Assis Peixoto[1]

Received: 27 December 2018 / Accepted: 11 November 2019

Abstract

Purpose The retina features the only blood vessel network in humans that is visible in a non-invasive imaging method. This, along with uniqueness and stability throughout life in healthy subjects, makes it an ideal target for personal identification methods in biometric systems and also for the screening and diagnosis of diseases. However, retinal images usually present low contrast of the vessels in relation to the retinal background and high level of noise stemming mainly from the acquisition process. This work aims to reduce noise and improve contrast to increase the accuracy of retinal vessel segmentation.

Methods 2D Gabor wavelet (GW) is usually employed to reduce noise and improve vessel contrast in relation to the background. In this work, it is proposed that, before the thresholding, the GW output images are partitioned into 20 sub-images in such a way that each can be treated independently.

Results The images used were obtained from two public databases, DRIVE and STARE, and the algorithm was developed in MatLab® environment. The proposed approach reached an accuracy of 96.15%, sensitivity of 73.42%, and specificity of 98.30% in DRIVE. In STARE, the accuracy was 94.87%, sensitivity 71.74%, and specificity 96.93%.

Conclusion The methods proposed by the authors indicate gains in accuracy and specificity in the automatic detection of retinal vessels, in both databases used, when compared with those in the main published works. The accuracy is also higher than the 94.73% in interobserver accuracy previously determined as the gold standard.

Keywords Low contrast · Denoising · 2D Gabor wavelet · Image partitioning · Image thresholding · Segmentation of retinal vessels

Introduction

The study of retinal blood vessels has generated great interest in current research. It represents a reliable source for systems that use biometrics (Akram et al. 2011; Fatima et al. 2013; Waheed et al. 2015) since these vessels are visible in a non-invasive imaging method (Fraz et al. 2014) and are unique and stable throughout life in healthy subjects (Akram et al. 2011).

Retinal blood vessels can also be used for screening and diagnosis of several diseases (Abramoff et al. 2010), including diabetic retinopathy, the leading cause of blindness in working-aged people. This disease alone is responsible for close to 5 million cases of blindness each year, all of which are potentially preventable (World Health Organization 2019). The analysis of the retinal blood vessels is, therefore, of vital importance (Haleem et al. 2015).

The current clinical practice is that retinal images are taken through a procedure called retinography, usually performed by technicians. The acquired images are typically evaluated by an ophthalmologist, preferably one who is also a retina specialist, according to personal clinical experience. It has been shown that there is only mild interobserver reliability among

✉ Luciana da Silva Amorim
lucianamorimm@gmail.com

[1] Graduation Program in Electrical Engineering, Pontifical Catholic University of Minas Gerais - PUC-MG, Belo Horizonte, Itau Avenue, 525, Dom Cabral, Belo Horizonte, MG CEP 30535-012, Brazil

[2] Dr. Ricardo Guimarães Eye Hospital, Belo Horizonte, MG, Brazil

Published online: 30 November 2019

ophthalmologists, nurses, and ophthalmic photographers (Ruamviboonsuk et al. 2006) and even doctors who may be diabetes specialists but not ophthalmologists commit a high rate of serious diagnostic errors, reaching up to 50% (Lienert 1989).

Manual segmentation is highly time-consuming, demands proper training, and involves subjective analysis from those who perform it (Ali et al. 2017). It is reasonable to expect that fatigue of human observers might cause a loss in segmentation precision over time in real-life scenarios (Niemeijer et al. 2004).

Thus, automatic detection becomes a necessary and indispensable tool in these processes, for it would be an invaluable contribution if we consider the large number of patients screened, the need for periodical exams (at least once a year per patient), and the high cost of a specialized professional.

The greatest difficulty encountered in automatic detection of blood vessels is that retinal images generally present low contrast of the vessels in relation to the background and high noise level, mainly stemming from the acquisition process (Ali et al. 2017; Gou et al. 2017; Miri and Mahloojifar 2009; Razban et al. 2016; Shahnazi et al. 2007). These images can be acquired through fundus image cameras used by ophthalmologists (Akram et al. 2011; Haleem et al. 2015), but illumination is often irregular (Ali et al. 2017). Moreover, pathologies may create "false" vessels, which introduce error into their standard structure (Ali et al. 2017; Razban et al. 2016). Even eyelashes, eyelids, or dust on the optic surface hinder proper vessel detection (Haleem et al. 2015).

Miri and Mahloojifar (2009) developed an algorithm for enhancing retinal image contrast with edge enhancement without noise amplification. This proposal is based on the second generation of the curvelet transform coefficients. The method developed by Akram et al. (2009) combines the 2D Gabor wavelet transform, hereafter referred to as of 2D Gabor wavelet or GW, which accentuates the vascularization pattern. As it results in a blurred image, a sharpening filter is used to improve that visualization by sharpening the edges. AlZaid et al. (2018) used Gabor filter for contrast enhancement. The appearance of the vessels is modified as this filtering uses the directional field method to determine the orientation of the image's scanning angle, which ranges from 0° to 180°.

In addition to the low contrast, estimating the width of the retinal vessels in the images with non-uniform contrast is another factor that hinders its extraction, especially for thinner vessels, which are difficult to detect. Gou et al. (2017) presented an extraction method that improves the detection of such thin vessels by determining scales for the Gaussian filter. The image is divided into sub-images of equal size and the scale of each sub-image is allocated according to the local histogram. Shahnazi et al. (2007) used wavelet energy feature (WEF) to distinguish vessels with different diameters. That choice is due to the WEF's ability to show the energy distribution in different directions and levels of wavelet decomposition of the vessels, allowing the correct identification and consequent segmentation.

In order to perform retinal vessel segmentation, Ali et al. (2017) proposed the combination of automatic threshold and 2D Gabor wavelet. The image from the green channel is used as input, and then the contrast-limited adaptive histogram equalization (CLAHE) algorithm is used followed by background normalization to enhance contrast. The output image of the CLAHE and the original green channel image are binarized after being processed by GW and combined using the OR logic operation in order to obtain a better vessel extraction. Morphological operations are employed to remove pixels detected wrongly. A similar proposal was presented by Nugroho et al. (2017). Initially, the green channel is extracted, and then a complement operation is applied followed by CLAHE and the opening operation. Next, the 2D Gabor wavelet is applied. The image binarization, closing operation, and morphological reconstruction of the vessels are performed based on the concept of dilation and connectivity. Razban et al. (2016) combined the 2D Gabor wavelet and fuzzy mathematical morphology, estimated the region of interest (ROI) through GW, and used fuzzy operations on the modified top-hat transform to segment the retinal vessels. The proposal in Soares et al. (2006) for segmentation was to classify each pixel as a vessel or background based on the pixel's characteristic vector. Those vectors are formed by the pixel intensity in the green channel and the GW responses and are calculated by varying the scale.

Veras et al. (2013) proposed an algorithm for the detection and segmentation of fat deposits in the retina, called exudates. Such fat deposits are a sign of diabetic retinopathy. The authors used the combination of mathematical morphology, nebulous grouping, and a stage of optical disc detection, which resulted in the elimination of false candidates for exudates and consequent improvement in the accuracy rate. The work of Arthur et al. (2017) consisted of an algorithm to identify macular dysfunction, as people with diabetes usually present changes in the foveal avascular zone (FAZ) prior to retinopathy. The descriptors used are based on Hu's moments invariant from the foveal avascular zone and the algorithm performs the automatic segmentation of that region, classifying it as normal (healthy) or abnormal (sick).

The articles by Akram et al. (2011), Fatima et al. (2013), and Waheed et al. (2015) performed the extraction of retinal blood vessel with the purpose of being used in the recognition of an individual. 2D Gabor wavelet was used in pre-processing for contrast enhancement and noise filtering, and then an adaptive threshold was applied for vessel segmentation. In Waheed et al. (2015), a vessel validation stage was incorporated based on characteristics such as shape and intensity.

The aim of this work is the automatic and precise segmentation of the retinal vessels based on the association of the 2D Gabor wavelet and the partitioning of the image before the

thresholding. In this way, it was possible to reduce the noise and improve the contrast, achieving greater segmentation accuracy in comparison with the main published related works. The proposed scheme comprises the stages in pre-processing, when the 2D Gabor wavelet is applied for contrast and noise filtering improvement, and the segmentation stage, where image partitioning and thresholding are performed using the Otsu. The proposed algorithm was developed in MatLab® environment and the images used were obtained from public databases, DRIVE and STARE. The results obtained were compared with the results presented by Soares et al. (2006), Akram et al. (2009), Ali et al. (2017), Gou et al. (2017), Nugroho et al. (2017), and AlZaid et al. (2018), proving the improvement in the specificity and accuracy criteria.

Methods

The process of extracting retinal blood vessels comprises the stages of pre-processing and segmentation, as shown in the methodology diagram in Fig. 1. Pre-processing aims to improve contrast and noise filtering. Segmentation, in turn, categorizes the image pixels into vessels or background.

The retinal images were obtained from two public databases named DRIVE and STARE. The images of DRIVE database were extracted through a screening program for diabetic retinopathy carried out in the Netherlands (Staal et al. 2004). This database provides 40 images: 20 for training and 20 for testing. It also supplies the manual segmentation of vasculature that is performed by professionals and a delimiting mask of the region corresponding to the field of view for all images. The STARE database consists of 400 retinal images and 20 manually segmented images (Hoover et al. 2000).

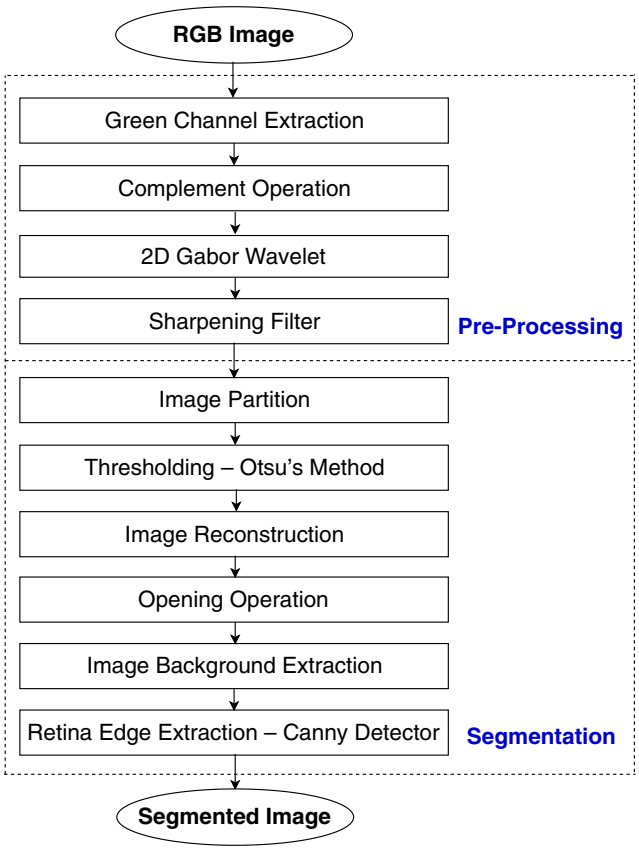

Fig. 1 Diagram of the proposed methodology

Pre-processing

The images provided by the databases are colored in RGB color space. By visual inspection, it can be observed that the green channel presents better contrast than the others, being preferably used in the segmentation processes in available literature, and also selected in this work (Akram et al. 2011; Ali et al. 2017; Fatima et al. 2013; Gou et al. 2017; Miri and Mahloojifar 2009; Nugroho et al. 2017; Razban et al. 2016; Soares et al. 2006). Figure 2 shows an original image, each of the RGB channels separately and each channel's corresponding histogram.

Note that the green channel histogram shown in Fig. 2c is bimodal, leading to the false assumption that global thresholding using the Otsu algorithm is sufficient for retinal vessel segmentation. However, it is important to observe that the image has a high noise level. The dark pixels in the histogram represent the background pixels of the image (which will be removed later) and, for the most part, the thicker vessels. Most of the fine vessels have medium gray intensity and present a lower contrast to the retinal background. Thus, applying the Otsu algorithm without the pre-processing step would segment satisfactorily only the thick vessels. This would reduce sensitivity and therefore accuracy. However, a processed image with lower noise content and sharper contrast between the thin vessels and the retinal background is required. The increase of thin vessel-background contrast can be obtained by applying the 2D Gabor wavelet transform, in the same way as the works of Akram et al. (2011), Akram et al. (2009), Ali et al. (2017), Fatima et al. (2013), Nugroho et al. (2017), Razban et al. (2016), Soares et al. (2006), and Waheed et al. (2015).

Before applying the Gabor wavelet transform, it is important to apply a complement operation on the green channel image so that the blood vessels are lighter than the background (Nugroho et al. 2017).

The Wavelet transform is a multiresolution analysis tool that allows us to decompose and represent a function in the space-frequency domain, in a two-dimensional case. The one-dimensional Gabor function consists of a complex exponential located around $x = 0$ and surrounded by a Gaussian window. The Gabor wavelets are then created by the dilation and

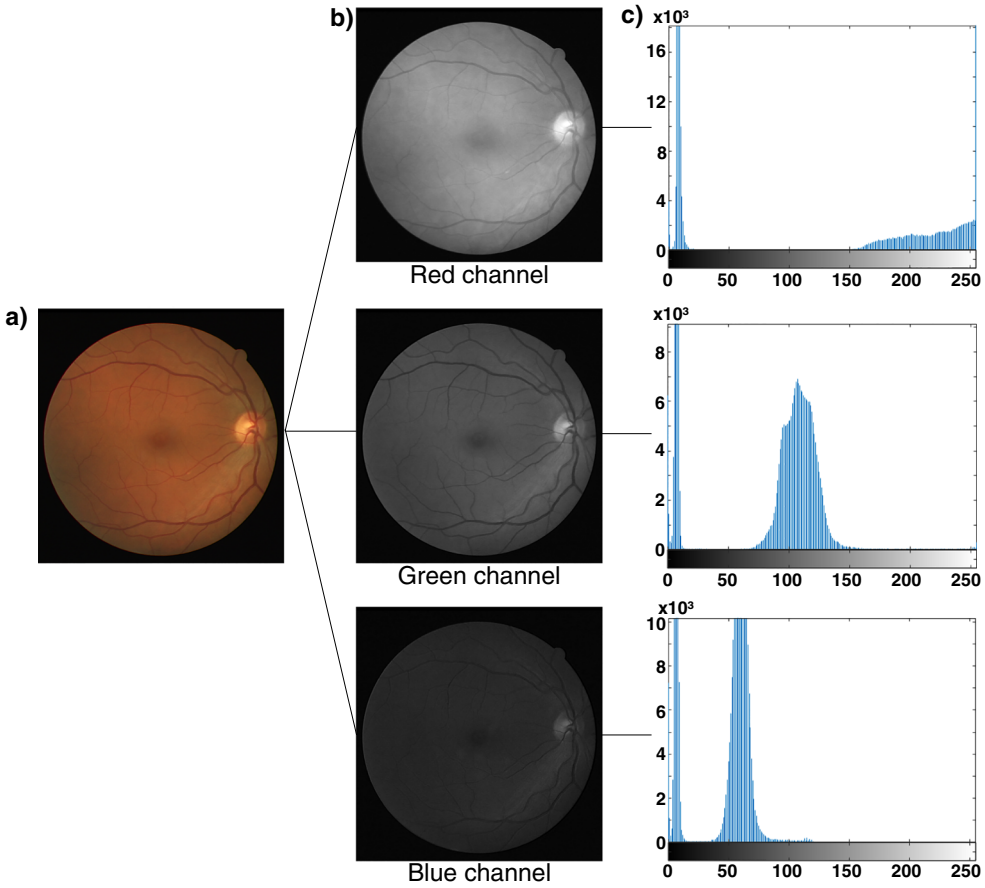

Fig. 2 Retinal image, color channels, and histograms. a) Original image. b) Separation of red, green, and blue channels. c) Histograms corresponding to each channel

displacement of the elementary function, called the mother wavelet (Bařina 2011).

The Gabor wavelet function of x is given by (Soares et al. 2006):

$$\psi_G(x) = \exp(jk_0x)\exp\left(-\frac{1}{2}|Ax|^2\right) \quad (1)$$

where k_0 is the frequency of the complex exponential and $A = \mathrm{diag}\left[\epsilon^{\frac{-1}{2}}, 1\right]$, $\epsilon \geq 1$ is a 2×2 diagonal matrix that defines the filter anisotropy.

The 2D Gabor wavelet transform performs noise filtering and edge enhancement, highlighting the hard-to-detect thinner vessels. This is made possible because the GW is tunable with any specific frequencies and orientations (Soares et al. 2006). In the analysis, the signals are decomposed at different levels, allowing the separation of the noise from the signal of interest. By identifying the coefficients that present the maximum wavelet response and applying thresholds for the selection of those coefficients, it is then possible to filter the noises (Kim and Aggarwal 2001). In the synthesis stage, the filtered signal is recovered and then can be enhanced for better performance in the segmentation process.

The GW scale parameter was set at 4, as in the works of Akram et al. (2011), Ali et al. (2017), Fatima et al. (2013), and Soares et al. (2006). The Gabor wavelet transform was calculated for orientations between 0° and 170°, with steps of 10°, resulting in 18 images.

After the pre-processing stage, the resulting images are subjected to a sharpening filter with the Matlab® "imsharpen" function, as the resulting Gabor images might have been blurred (Akram et al. 2009).

Segmentation

Although the association of the wavelet transform and the sharpening filter results in improved contrast of the blood vessels with the background, the large vessels still have high wavelet response compared with the thin vessels (Fatima et al. 2013). As a solution proposed in this work, based on Gou et al. (2017), the filtered images of the GW output are partitioned before the thresholding. Thus, each one of the 18 resulting images of Gabor is divided into 20 sub-images, for which the threshold is calculated independently using the Otsu method. Figure 3 illustrates the application of the proposed partition.

After the thresholding, an image is formed for each orientation by joining the 20 sub-images. Then, the resulting image is formed by the overlapping of the 18 images in the 18 orientations.

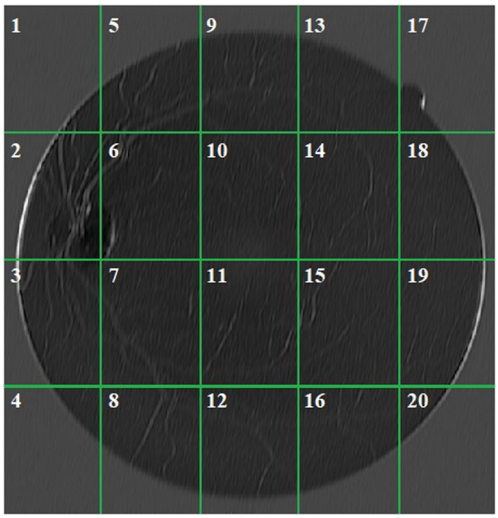

Fig. 3 2D Gabor wavelet transform output image for a 170° orientation after the sharpening filter, partitioned into 20 sub-images

The resulting image of the thresholding still contains some unwanted pixels that can be misclassified as vessels. To avoid this error, an opening morphological operation is performed to remove those pixels.

For the detection of the retinal edge, the Canny detector was used according to the following steps (Akram et al. 2009): (1) The Canny detector is applied to the original image, converted to shades of gray, and it returns the binarized image; (2) The vessels are dilated and then a background pixel filling operation of the object is performed, for the purpose of eliminating noise; (3) the perimeter of the object in the image is determined, i.e., the edge of the retina. The pixels external to the retina and the border are identified and classified as background.

For the DRIVE database, the mask that delimits the region of the retina in the image is already provided, whereas for the STARE base, it must be calculated. In both cases, the pixels corresponding to the blood vessels were given a value "1" and the pixels of the background were assigned a value "0."

Figure 4 illustrates the complete flowchart of the proposed retinal vessel segmentation process. Although there are 18 images resulting from the Gabor transformation, due to space limitation, only the image in direction 170° is shown. It is worth mentioning that the Otsu algorithm is applied to each of the sub-images before reconstruction.

Results and discussion

In the pre-processing stage, the extraction of the green channel is made from the original RGB image of the retina and then, the complement operation is applied to it highlighting the blood vessels. Next, the Gabor wavelet transform provides 18 images, which are individually taken to the segmentation stage after being submitted to sharpening filters.

Partitioning into sub-images before thresholding yielded improvements in the segmentation process. The global segmentation without partitioning and the final segmentation here obtained after including the partitioning of the images are shown in Fig. 5, where we can observe that the partition contributed to the detection of thinner vessels. Figure 5 also

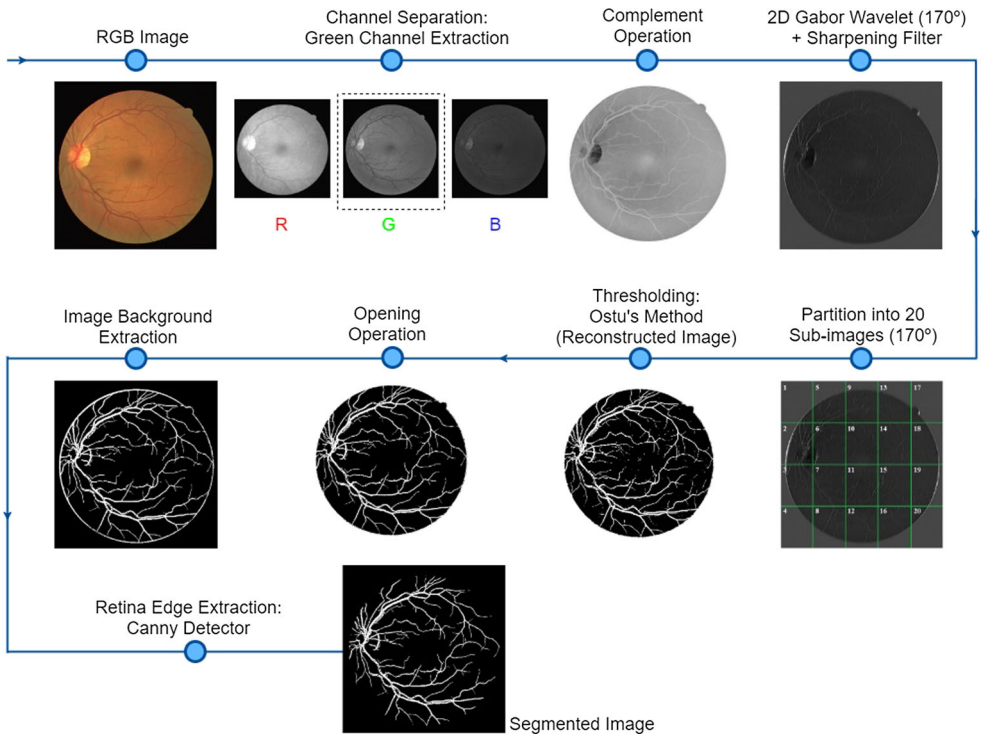

Fig. 4 Illustrative flowchart of the proposed retinal vessel segmentation

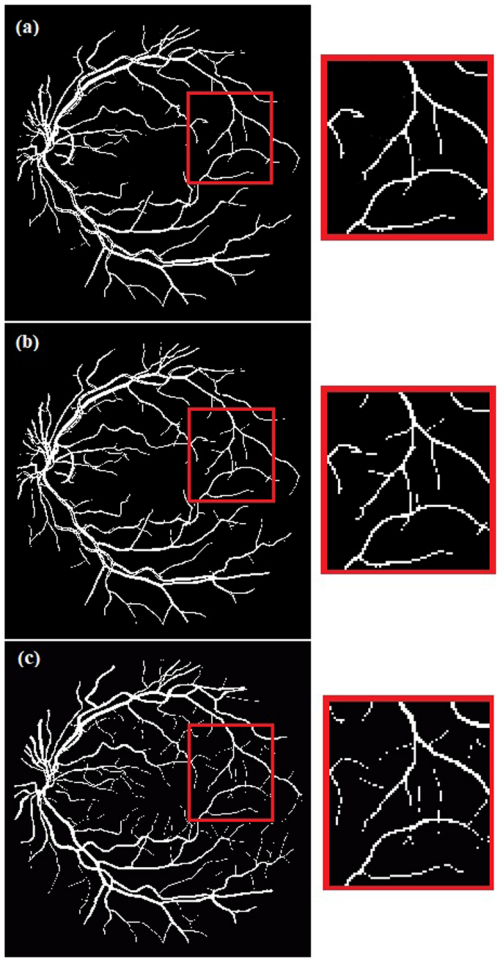

Fig. 5 Segmented image. **a** Automatically segmented image without image partition. **b** Image segmented automatically with partition. **c** Image segmented manually by a professional

shows the manual segmentation of the image performed by a professional.

The evaluation of the segmentation obtained is performed by comparing the automatically segmented image with the manually segmented image, pixel by pixel, which is taken as a reference. Most classified as vessels or as background and counted as true-positives T_p, true-negatives T_n, false-positives F_p, and false-negatives F_n.

Based on these parameters, the precision of the algorithm is assessed by its accuracy, sensitivity, and specificity. Accuracy is the average precision rate of segmentation; sensitivity is the ratio between vessels detected correctly and the total number of vessels. Specificity is the ratio between the background pixels detected correctly and the total number of background pixels. The performance criteria are calculated according to Eqs. (2) to (4), respectively:

$$\text{Accuracy} = \frac{Tp + Tn}{Tp + Tn + Fp + Fn} \tag{2}$$

$$\text{Sensitivity} = \frac{Tp}{Tp + Fn} \tag{3}$$

$$\text{Specificity} = \frac{Tn}{Tn + Fp} \tag{4}$$

Table 1 shows a comparative analysis of the results from the DRIVE and STARE databases, with and without image partitioning before the thresholding according to the proposed method. All three metrics increased with the proposed method.

Table 2 shows the results obtained according to the proposal of this work for the bases DRIVE and STARE in comparison with related works, available in the current technical-scientific literature.

It can be observed that the proposed methodology achieves better levels for the specificity and accuracy in the two databases. The result for sensitivity, which is presented by Nugroho et al. (2017), is better for both bases.

Statistical tests were performed to prove the validity of those results. The hypothesis tests results are shown in Table 3, for which a Student's t test with a 95% confidence interval was performed between this study and the best results for the specificity, sensitivity, and accuracy of the related works. In the tests for specificity and accuracy, since the proposed method has surpassed the related works, null hypotheses were stated as the average values obtained from this proposed method being equal to the best result in each parameter attained in related works. The alternate hypotheses were that the average values achieved here were larger than the best values reported in the literature. This aims at checking whether the superiority of our method against the best related work is statistically significant. Instead, sensitivity of Nugroho et al. (2017) is still better compared with that of the proposed method. Therefore, null hypothesis was stated as the average value

Table 1 Comparison of results with and without image partition

DRIVE				STARE		
Method	Specificity (%)	Sensitivity (%)	Accuracy (%)	Specificity (%)	Sensitivity (%)	Accuracy (%)
Without image partition	97.27	70.50	95.19	95.61	70.58	89.92
Proposed	98.30	73.42	96.15	96.93	71.74	94.87

Table 2 Comparison of results obtained from the proposed algorithm and other related works

	DRIVE			STARE		
Method	Specificity (%)	Sensitivity (%)	Accuracy (%)	Specificity (%)	Sensitivity (%)	Accuracy (%)
Soares et al. (2006)	–	–	94.66	–	–	94.80
Akram et al. (2009)	–	–	94.69	–	–	–
Ali et al. (2017)	97.85	72.11	94.53	–	–	–
Gou et al. (2017)	96.43	74.81	94.53	–	–	–
Nugroho et al. (2017)	97.13	80.75	95.87	90.45	90.45	89.46
AlZaid et al. (2018)	97.20	70.41	94.88	–	–	–
Proposed	98.30	73.42	96.15	96.15	96.93	94.87

being the sensitivity value achieved by the proposed method and alternate hypothesis was formulated as Nugroho et al. (2017) providing larger sensitivity than that.

To assert that one method is statistically different from the other, the p value (significance probability) should be less than 0.05 (for a 95% confidence interval). In Table 3, we can observe that this work presents more relevant results in specificity for the two databases and in accuracy for the DRIVE database. As for the accuracy in the STARE database, it cannot be stated statistically that this work is better than that of Soares et al. (2006). Nugroho et al. (2017) presents better sensitivity for both databases, at the expense of reducing accuracy.

Nugroho et al. (2017) presents better sensitivity because it was better at detecting pixels in the thinner vessels. This raises a problem by decreasing accuracy since it increases the number of false-positives (non-existent vessels) detected. This might be especially troublesome in the screening of diseases since the most common retinopathies such as in diabetes and hypertensive retinopathy and, other cardiovascular diseases evolve with a decrease in the number or the caliber of retinal vessels. In these scenarios, the higher number of false-positives might represent an inability to detect an abnormal exam and would, therefore, be ineffective in improving clinical outcomes.

Sensitivity is the lowest metric in all algorithms because the contrast between the vessels and the background is low and the image is noisy. The thinner vessels, in particular, are the most difficult to detect because they are thinner and have lower contrast. All works listed in Table 2 seek to solve this problem, especially Gou et al. (2017), who developed a segmentation method thinking precisely of the detection of smaller vessels. In general, it is not possible to sufficiently enhance these vessels and filter out the noise at the same time, which leads to a compromise of accuracy. Note also that the sensitivity obtained from the proposed methodology has results compatible with other proposals available in the literature (it is the third most sensitive method as listed in Table 2).

To our knowledge, the only previously published work where a comparison was made between human-trained personnel and automatic segmentation was in Niemeijer et al. (2004). In this case, the maximum interobserver accuracy was 94.73%. Our results were, therefore, superior in both databases. Notice that the accuracy obtained in Nugroho et al. (2017) for STARE database, on the other hand, is less than 94.73%.

Table 3 Hypothesis tests: p value for specificity, sensitivity, and accuracy

Database	Specificity	Sensitivity	Accuracy
DRIVE	9.17 e-05	0.001370	0.008919
STARE	4.875 e-07	0.009787	0.447000

Conclusion

The proposed method is an algorithm capable of minimizing noise and enhancing contrast in retinal images, thus achieving an efficient automatic segmentation of retinal vessels. This improvement was obtained through a partition of the original image into smaller parts in 18 GW orientations and by applying a sharpening filter before the global Otsu thresholding in each sub-image, consequently improving vessel detection.

In comparison with the main published works, the proposed method represents gains in accuracy and specificity when tested with the DRIVE and STARE public image databases. The same is true for the comparison between human-trained personnel and the automatic algorithm proposed in this article.

We suggest as an improvement to previously established methods the insertion of the additional step of image partitioning into these GW orientations before the thresholding

in vessel segmentation techniques. The tests we performed confirmed that this additional step increases accuracy, sensitivity, and specificity.

Acknowledgments The authors would like to thank JJ Staal, AD Hoover, and their colleagues for making their databases publicly available and the Laboratory of Applied Research in Neuroscience of Vision (LAPAN) along with Dr. Ricardo Guimarães Eye Hospital for the technical support.

Funding information This study was financed in part by the CAPES - Brazil - Finance Code 001.

References

Abramoff MD, Garvin MK, Sonka M. Retinal imaging and image analysis. IEEE Rev Biomed Eng. 2010;3:169–208. https://doi.org/10.1109/RBME.2010.2084567.

Akram MU, Tariq A, Nasir S, Khan AS. Gabor wavelet based vessel segmentation in retinal images. In: IEEE symposium on computational intelligence for image processing; 2009 Mar 30 - Apr 2; Nashville, United States of America. USA: IEEE; 2009. p. 116–9. https://doi.org/10.1109/CIIP.2009.4937890.

Akram MU, Tariq A, Khan AS. Retinal recognition: personal identification using blood vessels. In: International conference for internet technology and secured transactions; 2011 Dec 11–14; Abu Dhabi, United Arab Emirates. USA: IEEE; 2012; 2011. p. 180–4.

Ali A, Hussain A, Wan Zaki WMD. Vessel extraction in retinal images using automatic thresholding and Gabor wavelet. In: 39th Annual international conference of the IEEE engineering in medicine and biology society (EMBC); 2017 Jul 11–15; Seogwipo, South Korea. USA: IEEE; 2017. p. 365–8. https://doi.org/10.1109/EMBC.2017.8036838.

AlZaid E, Shalash WM, Abulkhair MF. Retinal blood vessels segmentation using Gabor filters. In: 2018 1st international conference on computer applications information security (ICCAIS); 2018 Apr 4–6; Riyadh, Saudi Arabia. USA: IEEE; 2018. p. 1–6. https://doi.org/10.1109/CAIS.2018.8441937.

Arthur AM, Arthur R, Silva AG, Fouto MS, Iano Y, Faria J. Algorithm for predicting macular dysfunction based on moment invariants classification of the foveal avascular zone in functional retinal images. Rev Bras Eng Biomed. 2017;33(4):344–51. https://doi.org/10.1590/2446-4740.01417.

Bařina D (2011) Gabor wavelets in image processing. In: Proceedings of the 17th Conference STUDENT EEICT; Apr; Brno, Czech Republic. p. 522–526. arXiv:1602.03308v1.

Fatima J, Syed AM, Akram U. A secure personal identification system based on human retina. In: 2013 IEEE symposium on industrial electronics applications; 2013 Sep 22–25; Kuching, Malaysia. USA: IEEE; 2013. p. 90–5. https://doi.org/10.1109/ISIEA.2013.6738974.

Fraz MM, Rudnicka AR, Owen CG, Strachan DP, Barman SA. Automated arteriole and venule recognition in retinal images using ensemble classification. In: 2014 international conference on computer vision theory and applications (VISAPP). Portugal. USA: IEEE; 2015; 2014 Jan 05–08; Lisbon. p. 194–202. https://doi.org/10.5220/0004733701940202.

Gou D, Ma T, Wei Y. A novel retinal vessel extraction method based on dynamic scales allocation. In: 2017 2nd international conference on image, vision and computing (ICIVC). Chengdu, China. USA: IEEE; 2017 Jun 2–4. p. 145–9. https://doi.org/10.1109/ICIVC.2017.7984535.

Haleem MS, Han L, Jv H, Li B. Fleming a. retinal area detector from scanning laser ophthalmoscope (SLO) images for diagnosing retinal diseases. IEEE Journal of Biomedical and Health Informatics. 2015;19(4):1472–82. https://doi.org/10.1109/JBHI.2014.2352271.

Hoover AD, Kouznetsova V, Goldbaum M. Structured analysis of the retina [internet]. California, United States of America; 2000. [cited 2018 Jul 20]. Available from: http://cecas.clemson.edu/~ahoover/stare/.

Kim CH, Aggarwal R. Wavelet transforms in power systems II examples of application to actual power system transients. Power Engineering Journal. 2001;15(4):193–202. https://doi.org/10.1049/pe:20010404.

Lienert RT. Inter-observer comparisons of ophthalmoscopic assessment of diabetic retinopathy. Aust N Z J Ophthalmol. 1989;17(4):363–8. https://doi.org/10.1111/j.1442-9071.1989.tb00555.x.

Miri MS, Mahloojifar A. A comparison study to evaluate retinal image enhancement techniques. In: 2009 IEEE international conference on signal and image processing applications; 2009 Nov 18–19; Kuala Lumpur, Malaysia. USA: IEEE; 2010. p. 90–94. https://doi.org/10.1109/ICSIPA.2009.5478726.

Niemeijer M, Staal J, Ginneken BV, Loog M, Abramoff MD. Comparative study of retinal vessel segmentation methods on a new publicly available database. In: Proc. Society of Photo-Optical Instrumentation Engineers (SPIE 5370); 2004 May 12. Medical Imaging: Image Processing; 2004. https://doi.org/10.1117/12.535349.

Nugroho HA, Lestari T, Aras RA, Ardiyanto I. Segmentation of retinal blood vessels using Gabor wavelet and morphological reconstruction. In: 2017 3rd International conference on science in information technology (ICSITech). Oct 25–26; Bandung, Indonesia. USA: IEEE; 2018; 2017. p. 513–6. https://doi.org/10.1109/ICSITech.2017.8257166.

Razban A, Mahjoory K, Nooshyar M. Segmentation of retinal blood vessels by means of 2D Gabor wavelet and fuzzy mathematical morphology. In: 2016 2nd International conference of signal processing and intelligent systems (ICSPIS). Dec 14–15; Tehran, Iran. USA: IEEE; 2017; 2016. p. 1–5. https://doi.org/10.1109/ICSPIS.2016.7869877.

Ruamviboonsuk P, Teerasuwanajak K, Tiensuwan M, Yuttitham K. Interobserver agreement in the interpretation of single-field digital fundus images for diabetic retinopathy screening. Ophthalmology. 2006;113(5):826–32. https://doi.org/10.1016/j.ophtha.2005.11.021.

Shahnazi M, Pahlevanzadeh M, Vafadoost M. Wavelet based retinal recognition. In: 2007 9th international symposium on signal processing and its applications. Sharjah, United Arab Emirates. USA: IEEE; 2008; 2007. p. 1–4. https://doi.org/10.1109/ISSPA.2007.4555369.

Soares JVB, Leandro JJG, Cesar RM, Jeline HF, Cree MJ. Retinal vessel segmentation using the 2-D Gabor wavelet and supervised classification. IEEE Trans Med Imaging. 2006;25(9):1214–22. https://doi.org/10.1109/TMI.2006.879967.

Staal JJ, Abramoff MD, Niemeijer M, Viergever MA, van Ginneken Bv. DRIVE: digital retinal images for vessel extraction [Internet]. The Netherlands. 2004 [cited 2018 Jul 20]. Available from: www.isi.uu.nl/Research/Databases/DRIVE/.

Veras RMS, Medeiros FNS, Araújo FHD, Santana AM, Silva RRV. Exudate detection in retina images by mathematical morphology techniques and fuzzy clustering. Rev Bras Eng

Biomed. 2013;29(1):45–56. https://doi.org/10.4322/rbeb.2013.003.

Waheed Z, Akram UM, Waheed A, Shaukat A. Robust extraction of blood vessels for retinal recognition. In: 2015 Second international conference on information security and cyber forensics (InfoSec); 2015 Nov 15–17; Cape Town, South Africa. USA: IEEE; 2016. p. 1–4. https://doi.org/10.1109/InfoSec.2015.7435497.

World Health Organization. Blindness and vision impairment prevention - priority eye diseases: Diabetic retinopathy. 2019. https://www.who.int/blindness/causes/priority/en/index5.html. Accessed 26 July 2019.